J. Fluid Mech. (1982), *vol.* 121, *pp.* 163–186
Printed in Great Britain

Steady thermocapillary flows in two-dimensional slots

By ASOK K. SEN† AND STEPHEN H. DAVIS

Department of Engineering Sciences and Applied Mathematics, The Technological Institute, Northwestern University, Evanston, Illinois 60201, U.S.A.

(Received 16 June 1981 and in revised form 13 November 1981)

Liquid in a slot flows owing to a temperature gradient applied along its free surface. The thermal variation of surface tension induces a steady viscous flow directed on the surface from hot to cold, and recirculating below. For small aspect ratios A, giving flow in thin, two-dimensional slots, an asymptotic theory valid for $A \to 0$ is used to obtain the fluid and thermal fields as well as the interfacial shapes. Solutions are obtained for both fixed lines and fixed angles at the contact between the interface and the solid side walls.

1. Introduction

Whenever a temperature gradient is imposed along the (sufficiently clean) interface between two immiscible fluids, motion results. This thermocapillary effect is induced from the balance on the interface of the jump in bulk shear stress and the surface-tension gradient along the interface. This interfacial stress is transmitted to the bulk by viscous forces.

Forced thermocapillary flows occur in many combustion configurations in which a flame propagates over a liquid fuel. Here the large temperature gradient along the fuel surface and the thermocapillary flow generated can control the characteristics of the flame by controlling the fuel-mixing properties (see e.g. Sirignano & Glassman 1970; Torrance 1971). Perhaps the simplest such flame-induced motion involves the flow of molten paraffin near the wick of a burning candle (Adler 1970). Clearly, a similar configuration is one involving a spot weld, where a liquid-metal pool is formed by a heat source. Although the material properties of the fluid are different, thermocapillary effects should be involved under similar conditions.

Thermocapillary flows are known to be important in the containerless processing of single crystals. Consider the configuration shown in figure 1 in which a cylindrical solid passes through a heating coil, melts, and then resolidifies into a single crystal of (it is to be hoped) high quality. The nature of the crystal formed depends on the local nature of the thermal, concentration and fluid-flow fields, so that there is a strong coupling between the fluid dynamics and the growth dynamics of the crystal. Even if the melt consists of a single component, and gravity is absent, there is a thermal-convection field in the melt (as shown), which is driven by variations in the surface tension with the temperature.

Steady thermocapillary flows in thin horizontally unbounded regions have been examined by Levich (1962), Birikh (1966), Yih (1968, 1969) and Adler & Sowerby (1970) using lubrication approximations (implicitly or explicitly) to simplify the

† Present address: Department of Mathematical Sciences, Indiana University – Purdue University at Indianapolis, Indianapolis, IN 46205, U.S.A.

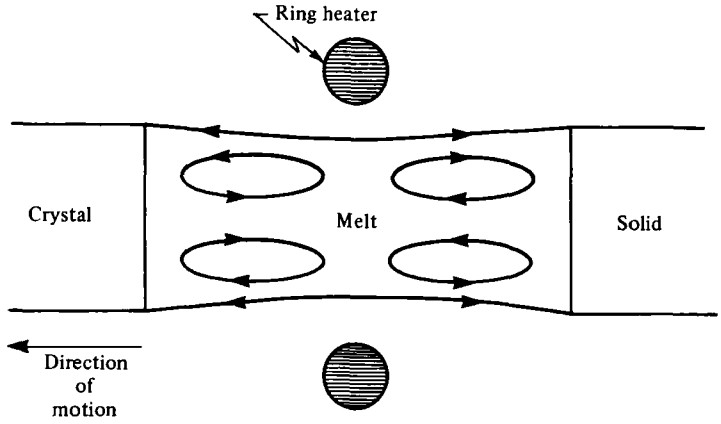

FIGURE 1. Schematic drawing of a float-zone processing configuration. The indicated convective flow (in the absence of gravity) is driven by thermal gradients in surface tension along the (liquid) melt–gas interface.

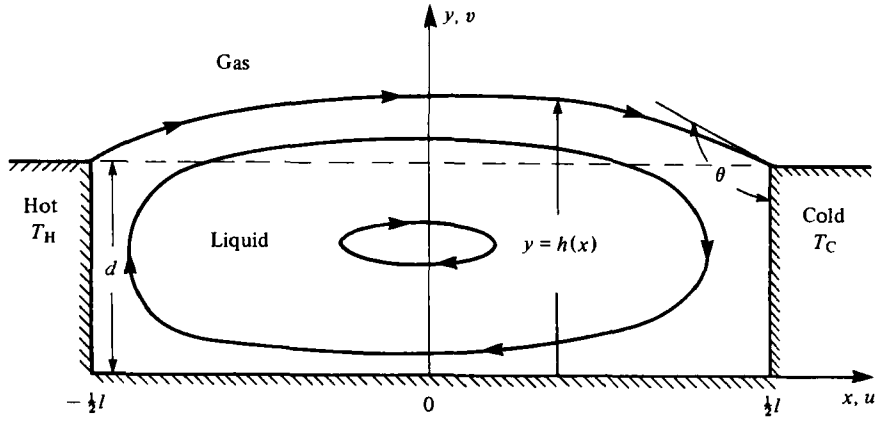

FIGURE 2. Schematic drawing of a two-dimensional slot flow having one liquid–gas interface and fixed side-wall contact lines (case I). The horizontal temperature difference $T_H - T_C$ is fixed and the lower boundary is a thermal insulator.

analyses. The only published work on such flows in bounded regions is due to Babskiy, Sklovskaya & Sklovskiy (1973), who consider a flow in a slot of unit aspect ratio. Ostrach (1977) criticizes this solution and further gives an overview of thermocapillary flows in general.

In order to study steady thermocapillary flows in bounded geometries we consider the two-dimensional layer of liquid shown in figure 2. Here the liquid is confined within a slot, which is differentially heated as shown. The differential heating induces a temperature gradient along the liquid–gas interface between the liquid and the gas, which in turn induces a surface-tension gradient along the interface. Since the length l of the layer is finite, conservation of mass requires the near-surface flow to turn around near the ends and recirculate below.

In the regions away from the ends, the flow *may* be relatively simple, but this flow cannot be fully determined without two additional considerations. First, the flow in the end regions must be analysed in order to relate the near-surface flows to the deeper return flows. Secondly, in problems of this type the interface is *not flat*. This is because

on one hand the flow dynamics is not compatible with a planar interface (Davis, Liu & Sealy 1974), and on the other hand a planar interface may not be compatible with the contact angles (both static and dynamic) at the ends. In the end regions the fluid meets the solid at an angle θ as shown in figure 2. This *dynamic* contact angle may be less than, equal to, or greater than, 90°. It depends not only on the specific materials present but on the dynamics of the fluid flow. Its value can be part of the solution of this free-boundary problem. Thus we see that the turning flows, the flow in the core region, the interface shape, and the dynamic contact angle are all tightly coupled together, with the end flows playing a critical role.

In the present analysis we examine steady thermocapillary flows in shallow slots having the aspect ratio $A \to 0$. Here A is the ratio of the mean depth of the liquid to the slot length, so that our approximate scheme uses the lubrication approximation. Our analysis parallels that of Cormack, Leal & Imberger (1974), who consider buoyancy-driven convection in a slot formed by rigid boundaries. Our analysis includes the added complications of surface-tension gradients on deformable interfaces. We examine four different cases. We consider the flow shown in figure 2 with either the contact line (the line formed by the intersection of the interface and the side wall) fixed or the contact angle fixed. We consider a slot flow having two deformable interfaces rather than one solid and one fluid interface. Here we again consider either the contact lines fixed or the contact angles fixed. We determine in all cases the flow fields, the temperature fields and the interfacial shapes.

2. Mathematical formulation

Consider a rectangular cavity of length l and height d, as shown in figure 2. It contains an incompressible Newtonian liquid of density ρ, thermal diffusivity κ and kinematic viscosity $\nu = \mu/\rho$; μ is the dynamic viscosity. The end walls at $x = \pm \frac{1}{2}l$ are maintained at temperatures T_{H} and T_{C} respectively, with $T_{\mathrm{H}} > T_{\mathrm{C}}$; the lower surface ($y = 0$) of the cavity is thermally insulated. The upper surface, described by $y = h(x)$, is a free surface bounded by a passive gas of negligible density and viscosity. This free surface is associated with a surface tension σ, which depends on the local temperature.

In the absence of gravity the steady two-dimensional motion of the liquid is governed by the equations

$$u_x + v_y = 0, \tag{2.1a}$$

$$uu_x + vu_y = -\rho^{-1}p_x + \nu(u_{xx} + u_{yy}), \tag{2.1b}$$

$$uv_x + vv_y = -\rho^{-1}p_y + \nu(v_{xx} + v_{yy}), \tag{2.1c}$$

$$uT_x + vT_y = \kappa(T_{xx} + T_{yy}), \tag{2.1d}$$

where u and v are respectively the horizontal and vertical velocity components, p is the pressure and T is the temperature of the liquid. These equations are subject to the following boundary conditions:

$$u = v = 0, \quad T = T_{\mathrm{H}} \quad (x = -\tfrac{1}{2}l); \tag{2.2a}$$

$$u = v = 0, \quad T = T_{\mathrm{C}} \quad (x = \tfrac{1}{2}l); \tag{2.2b}$$

$$u = v = 0, \quad T_y = 0 \quad (y = 0); \tag{2.2c}$$

$$\left.\begin{aligned} v = uh_x, \quad & S_{ij}n_jn_i = \sigma K, \\ S_{ij}n_jt_i = \sigma_s, \quad & k_1T_n + k_{\mathrm{g}}(T - T_{\mathrm{g}}) = 0 \end{aligned}\right\} \quad (y = h(x)). \tag{2.2d, e, f, g}$$

Equation (2.2d) is the kinematic boundary condition at the liquid–gas interface. The stress balances at the interface in the normal and tangential directions are given respectively by (2.2e) and (2.2f). The jump in the normal stress across the interface is balanced by surface tension times curvature, and the jump in the shear stress equals the surface-tension gradient along the interface. In these equations S_{ij} are the components of the stress tensor of the liquid, defined by

$$S_{ij} = -p\delta_{ij} + 2\mu\epsilon_{ij}, \quad \epsilon_{ij} = \tfrac{1}{2}(u_{i,j} + u_{j,i}), \tag{2.3}$$

$\mathbf{u}$ being the velocity vector and δ_{ij} the Kronecker delta. The unit outward normal vector $\mathbf{n}$ and the unit tangent vector $\mathbf{t}$ are defined as follows:

$$\mathbf{n} = (-h_x, 1)/N, \quad \mathbf{t} = (1, h_x)/N, \tag{2.4}$$

with

$$N = (1 + h_x^2)^{\frac{1}{2}}. \tag{2.5}$$

The subscript s in (2.2f) denotes the directional derivative along the free surface and the curvature K in (2.2e) has the definition

$$K(h) = h_{xx}/N^3. \tag{2.6}$$

The thermal boundary condition at the interface is given by (2.2g), in which k_1 is the thermal conductivity of the liquid and k_g is the heat transfer coefficient in the gas; T_g is the temperature in the gas phase. The subscript n represents the normal derivative at the interface.

Apart from the boundary conditions (2.2), the velocity field must also satisfy the condition

$$\int_0^{h(x)} u(x, y)\, dy = 0, \tag{2.7}$$

which follows from the fact that there exists no net mass flow into and out of the cavity. Furthermore, since the liquid is assumed incompressible, its total volume must remain constant; as a consequence the relation

$$\int_{-\frac{1}{2}l}^{\frac{1}{2}l} h(x)\, dx = V \tag{2.8}$$

must hold, where V is the total (two-dimensional) volume occupied by the liquid.

Finally, to close the problem, we need to specify the type of contact made by the free surface at the end walls. We shall restrict ourselves to the following two cases.

Case I: The liquid sticks to a sharp edge at the end walls with

$$h(\pm \tfrac{1}{2}l) = d. \tag{2.9}$$

Case II: A contact angle θ is prescribed at each end wall so that

$$h_x(\pm \tfrac{1}{2}l) = \mp \tan(\theta - \tfrac{1}{2}\pi). \tag{2.10}$$

In order to determine the velocity and temperature fields in the liquid, the temperature distribution T_g in the overlying gas must be known *a priori*. We shall assume that the heated and cooled solid ends of the cavity induce a sensibly conduction-

dominated temperature in the gas so that a linear variation of temperature exists. This profile is given by

$$T_g = \tfrac{1}{2}(T_H + T_C) - (T_H - T_C)\,x/l. \tag{2.11}$$

The temperature boundary condition (2.2g) reflects the existence of a thin convective thermal boundary layer in the gas.

We shall use a linear equation of state for surface tension. In particular, we take

$$\sigma(T) = \sigma_0 - \gamma[T - \tfrac{1}{2}(T_H + T_C)], \tag{2.12}$$

where σ_0 is the surface tension of the liquid at the cavity centre, and the constant γ is the negative of the derivative of surface tension with respect to temperature.

We scale the problem in terms of lubrication-type variables by introducing the following primed quantities:

$$\left.\begin{aligned} &x = lx', \quad y = dy', \quad h = dh', \quad u = u_* u', \quad v = Au_* v', \\ &p = (\mu u_* l/d^2)\,p', \quad T - \tfrac{1}{2}(T_H + T_C) = (T_H - T_C)\,T', \quad \sigma = \sigma_0 \sigma', \end{aligned}\right\} \tag{2.13}$$

where the aspect ratio

$$A = d/l. \tag{2.14}$$

The characteristic velocity u_* is derived from the so-called Marangoni effect, i.e. the jump in shear stress along the interface balances the surface-tension gradient. Thus using

$$\mu u_y \sim \sigma_x = \left(\frac{d\sigma}{dT}\right) T_x$$

leads to

$$u_* = \gamma A(T_H - T_C)/\mu. \tag{2.15}$$

Note that, when the inertial effects are small, the appropriate scale for pressure is $\mu u_* l/d^2$.

With these scales, the dimensionless equations (with the primes dropped) can be written in the form

$$u_x + v_y = 0, \tag{2.16a}$$

$$RA(uu_x + vu_y) = -p_x + A^2 u_{xx} + u_{yy}, \tag{2.16b}$$

$$RA^3(uv_x + vv_y) = -p_y + A^2(A^2 v_{xx} + v_{yy}), \tag{2.16c}$$

$$MA(uT_x + vT_y) = A^2 T_{xx} + T_{yy}. \tag{2.16d}$$

The Reynolds number R and the Marangoni number M have the definitions

$$R = u_* d/\nu = \frac{\gamma A(T_H - T_C)\,d}{\mu\nu}, \tag{2.17}$$

$$M = u_* d/\kappa = \frac{\gamma A(T_H - T_C)\,d}{\mu\kappa}, \tag{2.18}$$

and

$$R = P^{-1}M, \tag{2.19}$$

where the Prandtl number P is given by

$$P = \nu/\kappa. \tag{2.20}$$

This type of scaling has been discussed by Ostrach (1977). The boundary conditions (2.2) transform to

$$u = v = 0, \quad T = \mp \tfrac{1}{2} \quad (x = \pm \tfrac{1}{2}); \tag{2.21a}$$

$$u = v = 0, \quad T_y = 0 \quad (y = 0); \tag{2.21b}$$

$$\left.\begin{aligned} v &= uh_x, && (2.21c)\\ -p + 2A^2(1+A^2h_x^2)^{-1}[(v_y - h_x u_y) + A^2 h_x(-v_x + h_x u_x)] & \\ = A^3 C^{-1} h_{xx}(1+A^2h_x^2)^{-\frac{3}{2}}(1 - A^{-1}CT), & && (2.21d)\\ (1-A^2h_x^2)(u_y + A^2 v_x) + 2A^2 h_x(v_y - u_x) & \\ = -(1+A^2h_x^2)^{\frac{1}{2}}(T_x + h_x T_y), & && (2.21e)\\ (1+A^2h_x^2)^{-\frac{1}{2}}(T_y - A^2 h_x T_x) + L(T+x) &= 0 && (2.21f) \end{aligned}\right\} \quad (y = h(x)).$$

In (2.21*d*), C is the capillary number, given by

$$C = \mu u_*/\sigma_0 = \gamma A(T_{\mathrm{H}} - T_{\mathrm{C}})/\sigma_0. \tag{2.22}$$

The capillary number measures the degree of deformation of the free surface, and $C \to 0$ implies that the mean surface tension is very large. The Biot number L is defined by

$$L = k_{\mathrm{g}} d/k_{\mathrm{l}} \tag{2.23}$$

and measures the heat transport between the gas and the liquid phases. The dimensionless forms of (2.7) and (2.8) are as follows:

$$\int_0^{h(x)} u\,dy = 0, \tag{2.24}$$

$$\int_{-\frac{1}{2}}^{\frac{1}{2}} h(x)\,dx = \overline{V}, \tag{2.25}$$

$$\overline{V} = V/dl. \tag{2.26}$$

The two cases of contact-line conditions are as follows:

$$h(\pm \tfrac{1}{2}) = 1, \tag{2.27}$$

$$h_x(\pm \tfrac{1}{2}) = \mp A^{-1} \tan(\theta - \tfrac{1}{2}\pi). \tag{2.28}$$

We eliminate the pressure from the momentum equations (2.16*b*, *c*) and introduce a stream function ψ such that

$$u = \psi_y, \quad v = -\psi_x. \tag{2.29a}$$

We obtain for the momentum equation

$$RA\{(\psi_y \psi_{xyy} - \psi_x \psi_{yyy}) + A^2(\psi_y \psi_{xxx} - \psi_x \psi_{xxy})\} = \psi_{yyyy} + 2A^2 \psi_{xxyy} + A^4 \psi_{xxxx}. \tag{2.29b}$$

For the present purpose we consider that the cavity has a small aspect ratio ($A \ll 1$). In particular, we treat the problem in the asymptotic limit $A \to 0$. In this limit (see Cormack *et al.* 1974) the entire flow field can be divided into two distinct regions: an outer (core) region away from the end walls where the flow is relatively simple, and an inner (boundary-layer) region near each end wall where the flow turns around, to conserve mass, and recirculates. The core flow, the shape of the interface and the turning flows are all coupled together. Therefore the complete flow structure

can only be determined by solving the flow in the inner and outer regions separately and then joining them by the use of an asymptotic matching procedure. This will be carried out in detail for the case where the liquid sticks to a sharp edge at the end walls. Results for other types of contact are presented later. Our analysis is based on the following asymptotic limits of the dimensionless parameters:

$$R = \bar{R}A, \quad M = \bar{M}A, \quad C = \bar{C}A^4, \quad L = O(1), \tag{2.30a–d}$$

with $\bar{R}$, $\bar{M}$ and $\bar{C}$ all $O(1)$. The limit $R = \bar{R}A$ is based on the assumption of slow liquid motion, so that to the leading approximation the inertial terms in the momentum equations do not play any role. The limit $M = \bar{M}A$ follows from the assumption that the Marangoni number is sufficiently small; as a result the convective terms in the energy equation can be ignored, to leading order. In particular, we consider small departure from the state of pure conduction. The combination $R = O(A)$ and $M = O(A)$ implies that the Prandtl number of the liquid is of order unity. Various other limiting values of R and M can be considered, corresponding to small and large values of the Prandtl number.

The distinguished limit $C = \bar{C}A^4$ on the capillary number is chosen rather carefully. It is found that a value of C larger than that given in (2.30*c*) results in a non-zero-mean plane Couette flow away from the walls; this is physically unacceptable since the core flow, to conserve mass, must reverse its direction somewhere along the vertical. On the other hand, if C is any smaller than the value prescribed in (2.30*c*), then the first non-trivial correction to the free-surface height from a flat interface appears at a higher order of approximation.

3. The outer (core) flow

In the work to be presented here, we consider the case where the liquid just fills the cavity so that $V = dl$ (i.e. $\bar{V} = 1$), and we prescribe the contact condition (2.27) of fixed position.

We look for a solution which, to a leading approximation, consists of a parallel flow in the core with a flat interface. Accordingly, we set the values given in (2.30) for the dimensionless parameters and write the expansions

$$\psi = \psi_0(y) + A\psi_1(x,y) + O(A^2), \tag{3.1a}$$

$$p = p_0(x,y) + Ap_1(x,y) + O(A^2), \tag{3.1b}$$

$$T = T_0(x,y) + AT_1(x,y) + O(A^2), \tag{3.1c}$$

$$h = 1 + Ah_1(x) + A^2h_2(x) + O(A^3). \tag{3.1d}$$

Substituting these in (2.29) and (2.16*d*) and the boundary conditions (2.21), we find to leading order

$$\psi_{0yyyy} = 0, \quad T_{0yy} = 0, \tag{3.2a, b}$$

with

$$\psi_0 = \psi_{0x} = 0, \quad T_0 = \mp\tfrac{1}{2} \quad (x = \pm\tfrac{1}{2}); \tag{3.3a}$$

$$\psi_0 = \psi_{0y} = 0, \quad T_{0y} = 0 \quad (y = 0); \tag{3.3b}$$

$$\left.\begin{aligned} \psi_{0x} = 0, \quad & -p_0 = \bar{C}^{-1}h_{1xx}, \\ \psi_{0yy} + T_{0x} = 0, \quad & T_{0y} + L(T_0 + x) = 0 \end{aligned}\right\} \quad (y = 1). \tag{3.3c, d / 3.3e, f}$$

We also have
$$\psi_0(1) = 0, \tag{3.4}$$
which follows from the condition (2.24) of zero mass flux, and the fact that $\psi_0(0) = 0$.

The solution for T_0 that satisfies (3.2*b*), (3.3*b*) and (3.3*f*) is simply
$$T_0 = -x, \tag{3.5}$$
so that the liquid temperature at leading order follows the gas temperature, independent of the Biot number.

The solution for ψ_0 satisfying (3.2*a*), (3.3*b*, *c*, *e*) and (3.4) is
$$\psi_0 = \tfrac{1}{4}y^2(y-1). \tag{3.6}$$
Clearly, the parabolic velocity field associated with ψ_0 is parallel to the bottom surface of the cavity; as a result, it cannot satisfy the boundary conditions (3.3*a*) prescribed at the end walls. This outer flow must therefore be joined (see Cormack *et al.* 1974) to the (non-parallel) turning flows at the ends using an asymptotic matching procedure. Note, however, that the temperature field T_0 satisfies the boundary conditions at both end walls, and consequently does not exhibit any boundary-layer behaviour at this order.

Use of the expression (3.6) for ψ_0 in the leading-order horizontal momentum equation (2.16*b*) shows that there exists a constant pressure gradient to leading order. In fact,
$$p_{0x} = \tfrac{3}{2}. \tag{3.7}$$
The condition (3.3*d*) then yields the interfacial-position perturbation
$$h_1 = (-\tfrac{1}{4}x^3 + H_1x^2 + H_2x + H_3)\bar{C}. \tag{3.8}$$
The constants H_1, H_2 and H_3 are to be determined by matching the two-term outer solution for h, namely $h \sim 1 + Ah_1$, with the corresponding inner solutions near the end walls, and using the condition
$$\int_{-\frac{1}{2}}^{\frac{1}{2}} h_{1c}(x)\,dx = 0. \tag{3.9}$$
This last condition has been obtained from (2.25). The subscript c in (3.9) refers to the uniformly valid composite expansion of the free-surface height h.

To the next order of approximation, the stream function and the temperature field satisfy the equations
$$\psi_{1yyyy} = 0, \quad T_{1yy} = 0, \tag{3.10a, b}$$
together with the boundary conditions
$$\psi_1 = \psi_{1x} = T_1 = 0 \quad (x = \pm\tfrac{1}{2}); \tag{3.11a}$$
$$\psi_1 = \psi_{1y} = T_{1y} = 0 \quad (y = 0); \tag{3.11b}$$
$$\left.\begin{aligned} &\psi_{1x} + \tfrac{1}{4}h_{1x} = 0, \quad -p_1 = \bar{C}^{-1}h_{2xx}, \\ &\psi_{1yy} + \tfrac{3}{2}h_1 = -T_{1x}, \quad T_{1y} + LT_1 = 0 \end{aligned}\right\} \quad (y = 1); \qquad \begin{aligned} &(3.11c, d) \\ &(3.11e, f) \end{aligned}$$
and the zero-mass-flux condition
$$\psi_1 + \tfrac{1}{4}h_1 = 0 \quad (y = 1). \tag{3.12}$$
In writing down (3.10)–(3.12), the expressions (3.5) and (3.6) for ψ_0 and T_0 have been used wherever appropriate. Note that the last condition (3.12) is an integrated form of the kinematic boundary condition (3.11*c*).

We find that
$$\psi_1(x,y) = -\tfrac{1}{4}h_1(x)y^3, \tag{3.13}$$
$$T_1(y) = 0. \tag{3.14}$$

In order to find h_1 we solve the $O(A)$ version of the momentum equation (2.16b), and find that
$$p_{1x} = -\tfrac{3}{2}h_1(x). \tag{3.15}$$

When form (3.15) is combined with condition (3.11d) we find that
$$h_{2xxx} = \tfrac{3}{2}\bar{C}h_1, \tag{3.16}$$
which can be integrated to yield
$$h_2 = \bar{C}\left[\frac{3}{2}\iiint h_1(x) + \kappa_1 x^2 + \kappa_2 x + \kappa_3\right]. \tag{3.17}$$

Once the solution for h_1 is known completely, the constants κ_1, κ_2 and κ_3 in (3.17) can be determined by matching the three-term outer solution for h with a three-term boundary-layer solution near each end wall and using the incompressibility condition
$$\int_{-\frac{1}{2}}^{\frac{1}{2}} h_{2o}(x)\,dx = 0. \tag{3.18}$$

Here $h_{2o}(x)$ forms part of the composite expansion for h which is uniformly valid throughout the entire length of the cavity.

Note that the velocity field given by (3.13) is strictly non-parallel. In fact, we shall see later that the stream function ψ_1 exhibits a two-cell structure. Since we are only interested in obtaining solutions that are correct to $O(A^2)$, it is not necessary to determine the higher-order approximations for ψ. However, in order to complete our analysis up to this order, an expression for $T_2(x,y)$ must be derived, since this will be needed in the calculation of the $O(A)$ boundary-layer stream functions near the end walls. The problem for T_2 is as follows:
$$T_{2yy} = -\tfrac{1}{4}\bar{M}y(3y-2); \tag{3.19a}$$
$$T_2 = 0 \quad (x = \pm\tfrac{1}{2}); \tag{3.19b}$$
$$T_{2y} = 0 \quad (y = 0); \tag{3.19c}$$
$$T_{2y} + LT_2 = 0 \quad (y = 1). \tag{3.19d}$$

This has the solution
$$T_2 = -\tfrac{1}{48}\bar{M}(3y^4 - 4y^3 + 1). \tag{3.20}$$

It is interesting to note that the temperature field, up to this order, is independent of the Biot number. Notice also that T_2 does not satisfy the thermal conditions at $x = \pm\frac{1}{2}$, so that thermal boundary layers must be present at this order.

4. Boundary-layer flows near the end walls

To determine the boundary-layer flow near the wall at $x = -\frac{1}{2}$, we stretch the x-co-ordinate and set
$$\xi = A^{-1}(\tfrac{1}{2} + x), \quad \eta = y. \tag{4.1}$$

This choice is dictated by the need to retain diffusion of heat and vorticity in both the x- and y-directions. In these variables, the equations for the stream function (2.29) and the temperature (2.16d) become

$$\nabla^4\psi = \bar{R}A[\psi_\eta(\psi_{\xi\eta\eta}+\psi_{\xi\xi\xi})-\psi_\xi(\psi_{\eta\eta\eta}+\psi_{\xi\xi\eta})], \tag{4.2a}$$

$$\nabla^2 T = \bar{M}A(\psi_\eta T_\xi - \psi_\xi T_\eta), \tag{4.2b}$$

where ∇^2 and ∇^4 are respectively the Laplacian and the biharmonic operators, with

$$\nabla^2 = \frac{\partial^2}{\partial\xi^2}+\frac{\partial^2}{\partial\eta^2}.$$

The associated boundary conditions (2.21) reduce to

$$\psi = \psi_\xi = 0, \quad T = \tfrac{1}{2} \quad (\xi = 0); \tag{4.3a}$$

$$\psi = \psi_\eta = 0, \quad T_\eta = 0 \quad (\eta = 0); \tag{4.3b}$$

$$\left.\begin{aligned} &\psi_\xi + \psi_\eta h_\xi = 0, && (4.3c)\\ &-p + 2A(1+h_\xi^2)^{-1}[(h_\xi^2-1)\psi_{\xi\eta} - h_\xi(\psi_{\eta\eta}-h_\xi\psi_{\xi\xi})] \\ &\qquad = A^{-3}\bar{C}^{-1}h_{\xi\xi}(1+h_\xi^2)^{-\frac{3}{2}}(1-A^3\bar{C}T), && (4.3d)\\ &(1-h_\xi^2)(\psi_{\eta\eta}-\psi_{\xi\xi}) - 4h_\xi\psi_{\xi\eta} = -A^{-1}(1+h_\xi^2)^{\frac{1}{2}}(T_\xi + h_\xi T_\eta), && (4.3e)\\ &(1+h_\xi^2)^{-\frac{1}{2}}(T_\eta - h_\xi T_\xi) + L[T-(\tfrac{1}{2}-A\xi)] = 0 && (4.3f) \end{aligned}\right\} \quad (\eta = h).$$

An appropriate set of matching conditions must be added to the above equations and the boundary conditions. The matching conditions are derived from the requirement that, for continuity in the flow structure, the flows in the core and the boundary layers must be smoothly connected. This leads to the conditions

$$\lim_{\xi\to\infty}\psi_{\mathrm{L}} = \lim_{x\to-\frac{1}{2}}\psi_{\mathrm{core}}, \tag{4.4a}$$

$$\lim_{\xi\to\infty}T_{\mathrm{L}} = \lim_{x\to-\frac{1}{2}}T_{\mathrm{core}} \tag{4.4b}$$

as $A\to 0$. The subscript L refers to the left-hand boundary layer near $x = -\frac{1}{2}$. Similar matching conditions apply at the right-hand boundary layer near $x = \frac{1}{2}$.

We now write the inner expansions

$$\psi = \tilde{\psi}_0(\xi,\eta) + A\tilde{\psi}_1(\xi,\eta) + O(A^2), \tag{4.5a}$$

$$p = \tilde{p}_0(\xi,\eta) + A\tilde{p}_1(\xi,\eta) + O(A^2), \tag{4.5b}$$

$$T = \tilde{T}_0(\xi,\eta) + A\tilde{T}_1(\xi,\eta) + A^2\tilde{T}_2(\xi,\eta) + O(A^3), \tag{4.5c}$$

$$h = 1 + A\tilde{h}_1(\xi) + A^2\tilde{h}_2(\xi) + O(A^3). \tag{4.5d}$$

Substitution of these expansions in (4.2) and the boundary conditions (4.3) results in the following leading-order problem:

$$\nabla^4\tilde{\psi}_0 = 0, \tag{4.6a}$$

$$\nabla^2\tilde{T}_0 = 0, \tag{4.6b}$$

with

$$\tilde{\psi}_0(0,\eta) = \tilde{\psi}_{0\xi}(0,\eta) = 0, \quad \tilde{T}_0(0,\eta) = \tfrac{1}{2}, \tag{4.6c}$$

$$\tilde{\psi}_0(\xi,0) = \tilde{\psi}_{0\eta}(\xi,0) = \tilde{T}_{0\eta}(\xi,0) = 0, \tag{4.6d}$$

$$\tilde{\psi}_{0\xi}(\xi,1) = 0, \quad \tilde{h}_{1\xi\xi}(\xi) = 0, \quad \tilde{T}_{0\xi}(\xi,1) = 0, \tag{4.6e–g}$$

$$\tilde{T}_{0\eta}(\xi,1) + L[\tilde{T}_0(\xi,1)-\tfrac{1}{2}] = 0. \tag{4.6h}$$

The appropriate matching conditions are

$$\lim_{\xi\to\infty}\tilde{\psi}_0(\xi,\eta)=\tfrac{1}{4}\eta^2(\eta-1),\quad \lim_{\xi\to\infty}\tilde{\psi}_{0\xi}(\xi,\eta)=0, \tag{4.7a, b}$$

$$\lim_{\xi\to\infty}\tilde{T}_0(\xi,\eta)=\tfrac{1}{2}. \tag{4.7c}$$

The conditions (4.7*a*, *b*) follow from matching $\tilde{\psi}_0$ with the outer solution (3.6), while the condition (4.7*c*) is obtained by matching $\tilde{T}_0$ with the leading-order outer solution (3.5) for temperature.

The solution for $\tilde{T}_0$ is easily written down:

$$\tilde{T}_0(\xi,\eta)\equiv\tfrac{1}{2}. \tag{4.8}$$

Before we can determine $\tilde{\psi}_0$, we must write down the system determining the next correction. This takes the form

$$\nabla^4\tilde{\psi}_1=\bar{R}[\tilde{\psi}_{0\eta}(\tilde{\psi}_{0\xi\eta\eta}+\tilde{\psi}_{0\xi\xi\xi})-\tilde{\psi}_{0\xi}(\tilde{\psi}_{0\eta\eta\eta}+\tilde{\psi}_{0\xi\xi\eta})], \tag{4.9a}$$

$$\nabla^2\tilde{T}_1=0, \tag{4.9b}$$

$$\tilde{\psi}_1(0,\eta)=\tilde{\psi}_{1\xi}(0,\eta)=\tilde{T}_1(0,\eta)=0, \tag{4.9c}$$

$$\tilde{\psi}_1(\xi,0)=\tilde{\psi}_{1\eta}(\xi,0)=\tilde{T}_{1\eta}(\xi,0)=0, \tag{4.9d}$$

$$\tilde{\psi}_{1\xi}(\xi,1)+\tilde{h}_1\tilde{\psi}_{0\xi\eta}(\xi,1)+\tilde{h}_{1\xi}\tilde{\psi}_{0\eta}(\xi,1)=0, \tag{4.9e}$$

$$\tilde{h}_{2\xi\xi}(\xi)=0, \tag{4.9f}$$

$$\tilde{T}_{1\xi}(\xi,1)=\tilde{\psi}_{0\xi\xi}(\xi,1)-\tilde{\psi}_{0\eta\eta}(\xi,1), \tag{4.9g}$$

$$\tilde{T}_{1\eta}(\xi,1)+L[\tilde{T}_1(\xi,1)+\xi]=0. \tag{4.9h}$$

In the above we have used the solution (4.8) where appropriate.

It is easy to see that we can determine $\tilde{T}_1$ as well:

$$\tilde{T}_1(\xi,\eta)\equiv-\xi. \tag{4.10}$$

The solutions (4.8) and (4.10) reflect the non-boundary-layer character of the temperature field, since

$$T\sim\tilde{T}_0+A\tilde{T}_1=\tfrac{1}{2}-A\xi=-x. \tag{4.11}$$

Given the form (4.10), the boundary conditions (4.6*e*) and (4.9*g*) combine to yield the simplified shear-stress condition

$$\tilde{\psi}_{0\eta\eta}(\xi,1)=1. \tag{4.12}$$

Thus, the problem for $\tilde{\psi}_0$ is given by (4.6*a*), the first two conditions of (4.6*c*, *d*), (4.7*a*, *b*) and (4.12).

For analysing the flow in the cold-wall boundary layer, we set

$$\zeta=A^{-1}(\tfrac{1}{2}-x),\quad \nu=y, \tag{4.13}$$

and write the expansions

$$\begin{aligned}
\psi&=\hat{\psi}_0(\zeta,\nu)+A\hat{\psi}_1(\zeta,\nu)+O(A^2),\\
p&=\hat{p}_0(\zeta,\nu)+A\hat{p}_1(\zeta,\nu)+O(A^2),\\
T&=\hat{T}_0(\zeta,\nu)+A\hat{T}_1(\zeta,\nu)+A^2\hat{T}_2(\zeta,\nu)+O(A^3),\\
h&=1+A\hat{h}_1(\zeta)+A^2\hat{h}_2(\zeta)+O(A^3).
\end{aligned} \tag{4.14}$$

Analogous to the solutions $\tilde{T}_0(\xi,\eta)$ and $\tilde{T}_1(\xi,\eta)$, the solutions for $\hat{T}_0(\zeta,\nu)$ and $\hat{T}_1(\zeta,\nu)$ can be obtained by writing the two-term outer solution $\bar{T} = -x$ in terms of the inner variables. This gives

$$\hat{T}_0(\zeta,\nu) = -\tfrac{1}{2}, \tag{4.15}$$

$$\hat{T}_1(\zeta,\nu) = \zeta. \tag{4.16}$$

We now find that the problem for $\hat{\psi}_0(\zeta,\nu)$ becomes identical to that for $\tilde{\psi}_0(\xi,\eta)$, if ξ is replaced by ζ and η by ν everywhere. It will therefore suffice to solve for $\tilde{\psi}_0$ only. Before proceeding with the derivation of the higher approximations to the stream functions, it is necessary to determine the shapes of the interface in these boundary layers.

We therefore consider the problem of finding the interface shape near the end walls, and in the process determine the unknown constants in the outer solutions (3.8) and (3.17) for h_1 and h_2. For the hot-wall boundary layer near $x = -\frac{1}{2}$, we solve (4.6f) subject to the boundary condition

$$\tilde{h}_1(0) = 0, \tag{4.17}$$

in case I, and the matching condition

$$\lim_{\xi\to\infty} \tilde{h}_1(\xi) = \bar{C}(\tfrac{1}{32} + \tfrac{1}{4}H_1 - \tfrac{1}{2}H_2 + H_3). \tag{4.18}$$

This last condition follows from matching two terms in the outer expansion of h with two terms in its inner expansion. The solution for $\tilde{h}_1$ is thus

$$\tilde{h}_1(\xi) \equiv 0, \tag{4.19}$$

with

$$\tfrac{1}{4}H_1 - \tfrac{1}{2}H_2 + H_3 = -\tfrac{1}{32}. \tag{4.20}$$

Similarly, in the boundary layer near $x = \frac{1}{2}$ we have

$$\hat{h}_{1\zeta\zeta} = 0, \tag{4.21a}$$

with

$$\hat{h}_1(0) = 0, \quad \lim_{\zeta\to\infty} \hat{h}_1(\zeta) = \bar{C}(-\tfrac{1}{32} + \tfrac{1}{4}H_1 + \tfrac{1}{2}H_2 + H_3). \tag{4.21b}$$

The solution for the system (4.21) is given by

$$\hat{h}_1(\zeta) \equiv 0, \tag{4.22}$$

and then

$$\tfrac{1}{4}H_1 + \tfrac{1}{2}H_2 + H_3 = \tfrac{1}{32}. \tag{4.23}$$

Since $\tilde{h}_1(\xi) = \hat{h}_1(\zeta) = 0$, the two-term outer expansion for h, namely

$$h \sim 1 + Ah_1(x), \tag{4.24}$$

where $h_1(x)$ is given by (3.8), is uniformly valid throughout the entire length of the cavity. Thus, using this as a composite expansion, we find from the incompressibility condition (3.9) that

$$\tfrac{1}{12}H_1 + H_3 = 0. \tag{4.25}$$

If we combine (4.20), (4.23) and (4.25), we find that

$$H_1 = 0, \quad H_2 = \tfrac{1}{16}, \quad H_3 = 0, \tag{4.26}$$

so that the perturbation of the free-surface height from a flat interface is given by

$$h_1(x) = -\tfrac{1}{4}\bar{C}x(x^2 - \tfrac{1}{4}). \tag{4.27}$$

The *outer expansion* for the stream function, correct to $O(A^2)$, can now be written from (3.6) and (3.13) as follows:

$$\psi \sim \tfrac{1}{4}y^2(y-1)+\tfrac{1}{16}A\bar{C}x(x^2-\tfrac{1}{4})\,y^3. \tag{4.28}$$

Proceeding in a similar manner, we find at the next order of approximation

$$\check{h}_2(\xi) = -\tfrac{1}{8}\bar{C}\xi, \quad \hat{h}_2(\zeta) = \tfrac{1}{8}\bar{C}\zeta, \tag{4.29}$$

together with

$$\kappa_1 = \frac{35\bar{C}}{35840}, \quad \kappa_2 = 0, \quad \kappa_3 = \frac{\bar{C}}{28672}. \tag{4.30}$$

As a result, the solution for $h_2(x)$ becomes

$$h_2(x) = -\frac{\bar{C}^2}{320}(x^2-\tfrac{1}{4})\,(x^4-x^2+\tfrac{5}{112}). \tag{4.31}$$

We now turn to the problem for $\check{T}_2$. This takes the form

$$\nabla^2\check{T}_2 = -\bar{M}\check{\psi}_{0\eta}, \tag{4.32a}$$

$$\check{T}_{2\eta}(\xi,0) = 0, \quad \check{T}_{2\eta}(\xi,1)+L\check{T}_2(\xi,1) = 0, \quad \check{T}_2(0,\eta) = 0, \tag{4.32b–d}$$

with

$$\lim_{\xi\to\infty}\check{T}_2(\xi,\eta) = -\tfrac{1}{48}\bar{M}(3\eta^4-4\eta^3+1), \tag{4.32e}$$

and we have used the form (3.20).

The problem for $\hat{T}_2(\zeta,\nu)$ is identical to the system (4.32) if $(\xi,\eta)\to(\zeta,\nu)$ and carets replace tildes.

We are now in a position to formulate the problem for $\check{\psi}_1$. The stream function satisfies (4.9*a*) subject to the first two conditions of (4.9*c*, *d*) and the conditions

$$\check{\psi}_{1\xi}(\xi,1) = 0, \tag{4.33}$$

$$\check{\psi}_{1\eta\eta}(\xi,1) = -\check{T}_{2\xi}(\xi,1), \tag{4.34}$$

with the matching conditions

$$\lim_{\xi\to\infty}\check{\psi}_1(\xi,\eta) = \lim_{\xi\to\infty}\check{\psi}_{1\xi}(\xi,\eta) = 0. \tag{4.35}$$

The condition (4.33) comes from the condition (4.9*e*) with $\check{h}_1(\xi)\equiv 0$, and the condition (4.34) comes from the shear-stress balance at $O(A^2)$ with $\check{h}_1(\xi)\equiv 0$. The conditions (4.35) are derived from matching two terms of the inner expansion $\psi\sim\check{\psi}+A\check{\psi}_1$ with its two-term outer expansion (4.28).

The problem for $\hat{\psi}_1(\zeta,\nu)$ in the cold-wall boundary layer is the same as that for $\check{\psi}_1(\xi,\eta)$ if $(\xi,\eta)\to(\zeta,\nu)$, $\partial/\partial\xi\to-\partial/\partial\zeta$ and carets replace tildes.

The problems for $\check{\psi}_0(\xi,\eta)$, $\check{\psi}_1(\xi,\eta)$ and $\check{T}_2(\xi,\eta)$ are now solved numerically to determine the flow structure near the hot boundary. The numerical scheme consists of a 13-point finite-difference approximation of the biharmonic operator and a 5-point approximation of the Laplacian. The boundary conditions at $\xi=\infty$ are applied at $\xi=5$. The finite-difference equations are solved using the method of successive over-relaxation to expedite convergence. The optimum value of the relaxation parameter ω_{opt} is chosen by trial and error for a fixed system of grid points. For the computation of $\check{\psi}_0(\xi,\eta)$, ω_{opt} is found to be 1·5; this value is used in all further computations of the

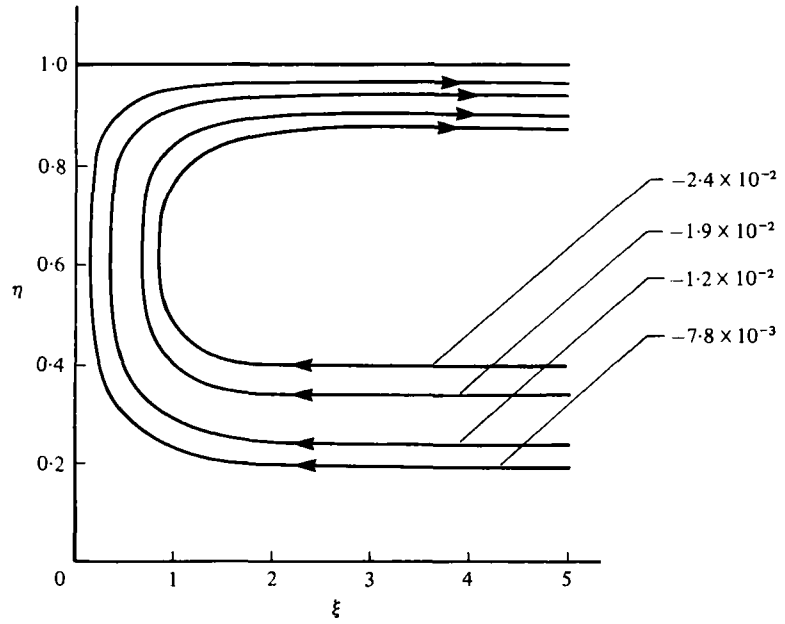

FIGURE 3. Leading-order streamlines in the left boundary layer with $L = 1$ for case I (and case II).

stream functions. The value of ω_{opt} for the calculation of $\hat{T}_2(\xi, \eta)$ is found to be 1·8. The results for case I are presented for the following set of parameter values:

$$A = 0{\cdot}2, \quad \bar{C} = 15, \quad L = 0 \text{ or } 1, \quad \bar{M} = 1, \quad \bar{R} = 5.$$

The large value of $\bar{C}$ is chosen for clarity of presentation. The numerically determined streamlines and the isotherms near the hot boundary are plotted in figures 3–5 for surface Biot number $L = 1$. It is clear from figure 3 that the streamlines are almost parallel for $\xi \geqslant 2$. This is to be expected, since the horizontal length scale that characterizes the flow near the end walls is comparable to the aspect ratio of the cavity. The stream functions $\hat{\psi}_0(\zeta, \nu)$, $\hat{\psi}_1(\zeta, \nu)$ and the temperature field $\hat{T}_2(\zeta, \nu)$ near the cold boundary are obtained by invoking the symmetry in the variables ξ and ζ. Given the boundary-layer solutions, we can construct the composite solutions valid for all $x \in [-\frac{1}{2}, \frac{1}{2}]$. Figure 6 shows these composite streamlines plus the interfacial shape correct to $O(A^2)$. Note the stretched scale in the drawing since $A = 0{\cdot}2$. The $O(A)$ streamlines, $\psi_1(x, y) =$ constant, are shown in figure 7. As noted above, these form a two-cell structure. The effect of variations in the capillary number $\bar{C}$ on the interfacial shape is shown in figure 8. As $\bar{C}$ increases, the surface tension decreases and the interface distorts further from the plane $y = 1$.

Computations similar to those above have been carried out for surface Biot number $L = 0$, the limiting case that represents a sharp mismatch between the thermal conductivities of the liquid and the gas. There are no qualitative changes in the solutions compared to the case with $L = 1$. For example the isotherms of figure 4 now intersect $y = 1$ at right angles, and are somewhat less densely bunched towards the upper left-hand corner. Since the range $L \in [0, 1]$ encompasses most physically relevant cases, we see that the thermal boundary condition only weakly influences the steady thermocapillary flow we examine.

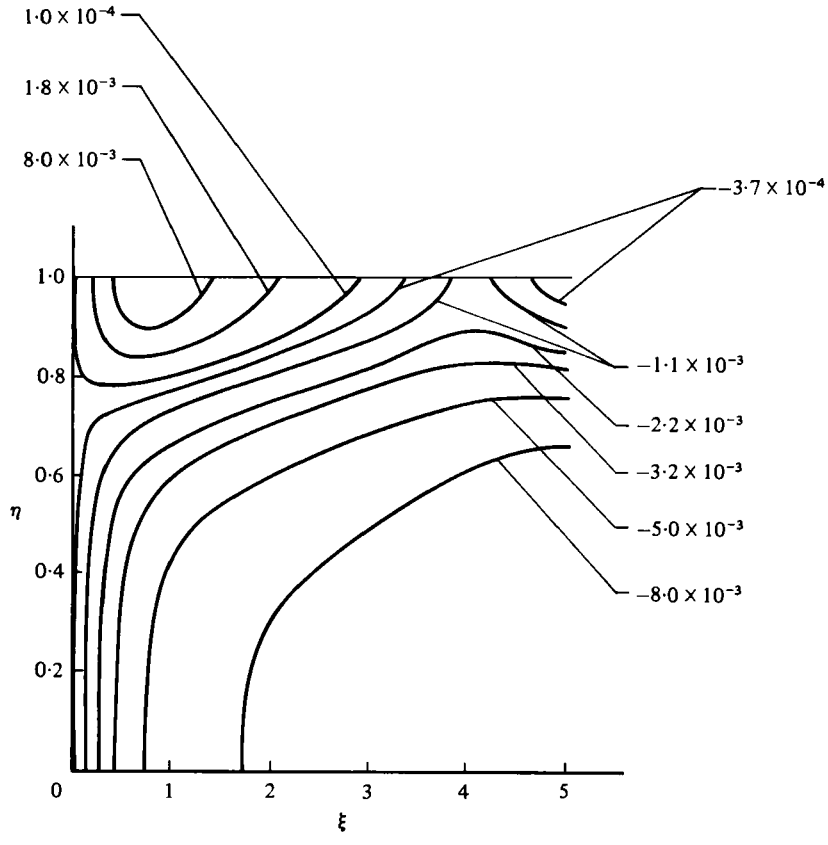

FIGURE 4. Order-A^2 isotherms in the left boundary layer with $L = 1$ for case I.

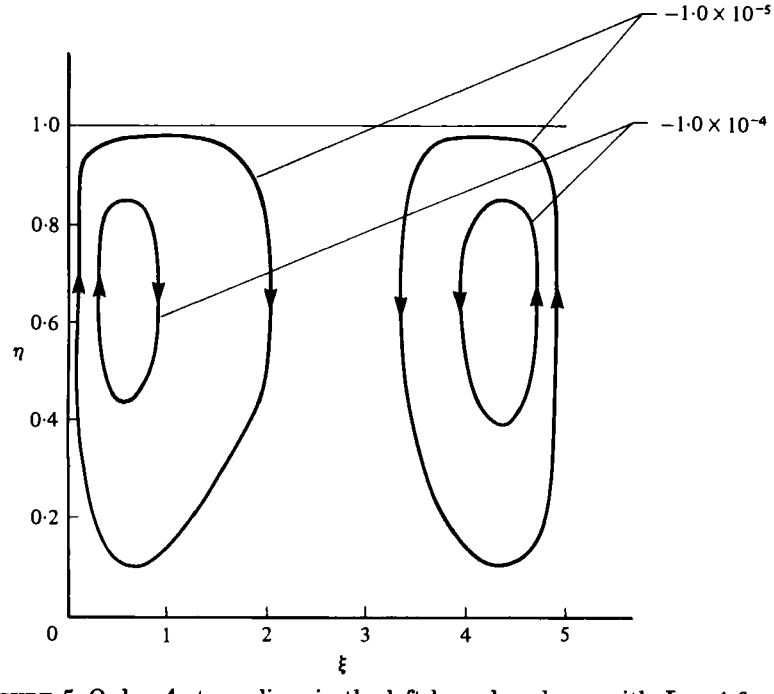

FIGURE 5. Order-A streamlines in the left boundary layer with $L = 1$ for case I.

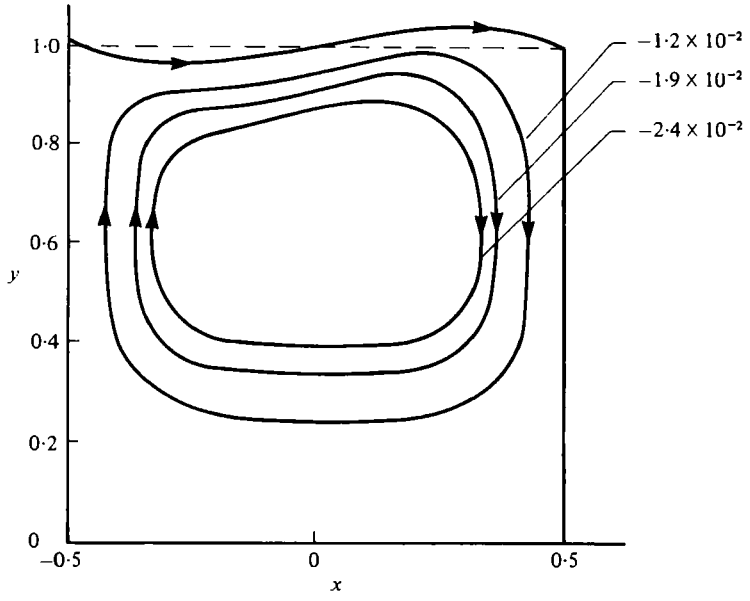

FIGURE 6. Composite streamlines and interface shape to order A^2 with $L = 1$ for case I.

5. Results for case II: prescribed contact angle

We consider the case of (2.28) with a contact angle θ near $\frac{1}{2}\pi$. We write†

$$\tan(\theta - \tfrac{1}{2}\pi) = mA^2\bar{C}, \quad m = O(1). \tag{5.1}$$

The contact line conditions (2.28)‡ now become

$$h'(\pm\tfrac{1}{2}) = \mp mA\bar{C}. \tag{5.2}$$

The analysis for this case is very similar to that for case I. We shall therefore present only the results. As in case I we look for a solution in which the interface is flat to a leading approximation, and find that the prescription (5.1) is consistent with such an assumption. If a value of m larger than that prescribed in (5.1) is used, a solution that has a flat top to a leading approximation cannot be found. The outer solutions for the stream function, temperature and the interface shape are given as follows:

$$\psi = \tfrac{1}{4}y^2(y-1) + \tfrac{1}{64}A\bar{C}\{x(4x^2-3) + \tfrac{4}{3}m(12x^2-1)\}y^3 + O(A^2), \tag{5.3a}$$

$$T = -x - \tfrac{1}{48}A^2\bar{M}(3y^4 - 4y^3 + 1) + O(A^3), \tag{5.3b}$$

$$h = 1 - \tfrac{1}{16}A\bar{C}\{x(4x^2-3) + \tfrac{4}{3}m(12x^2-1)\} + O(A^2). \tag{5.3c}$$

The boundary-layer problems for the stream function and the temperature for this case are analogous to those in case I. These are solved numerically using the same

† The form (5.1) is *not* a statement to the effect that the contact angle depends on A *physically* but that the mathematical order of magnitude of θ depends on A.

‡ We choose the contact angles at $x = \pm\frac{1}{2}$ to be equal. However, it is easy to allow different angles through different values of m for the two sides. This would for example allow one receding and one advancing angle to appear in the solution.

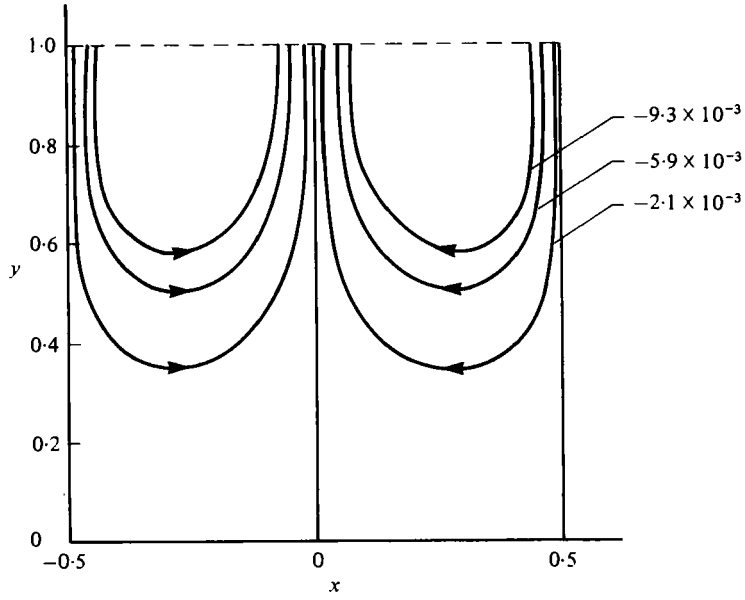

FIGURE 7. Order-A outer streamlines with $L = 1$ for case I.

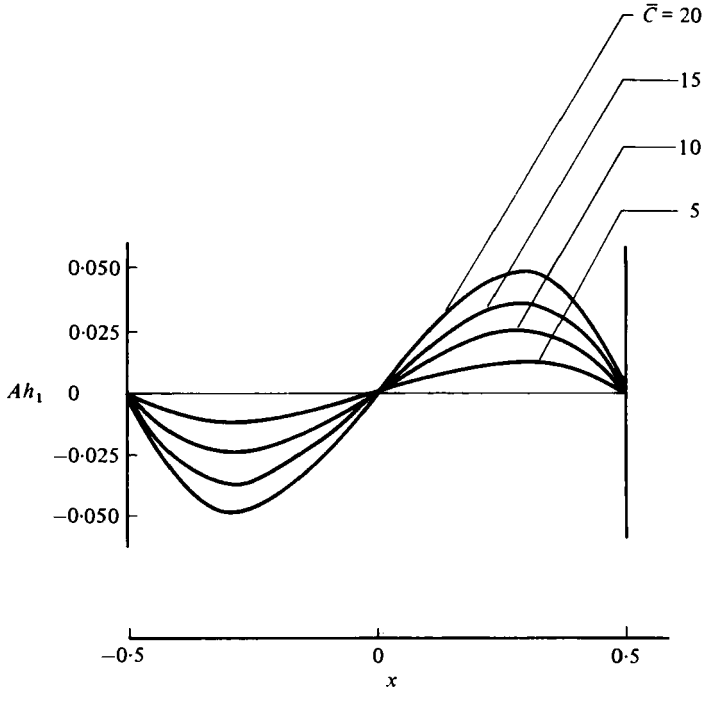

FIGURE 8. Effect of variations of capillary number on interface shape with $L = 1$ and $A = 0{\cdot}2$ for case I.

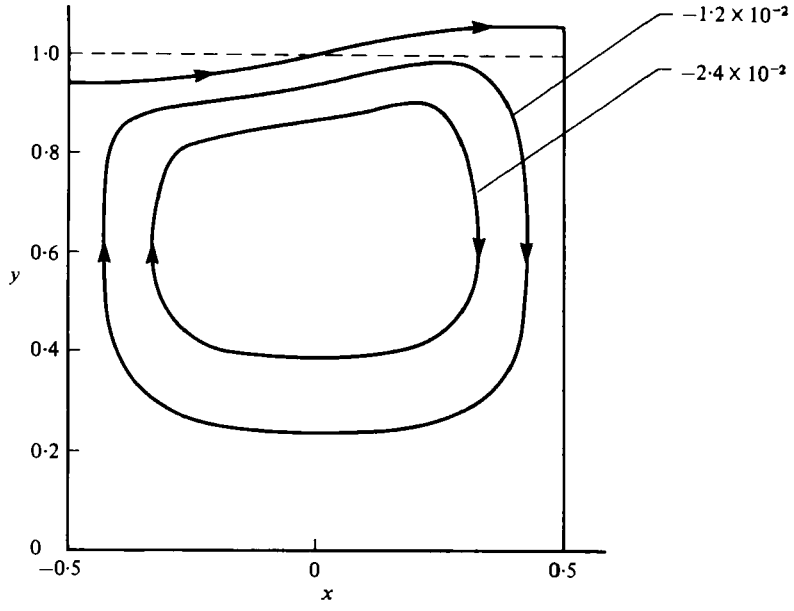

FIGURE 9. Composite streamlines and interface shape with $L = 1, A = 0{\cdot}2$ and $m = 0$ for case II.

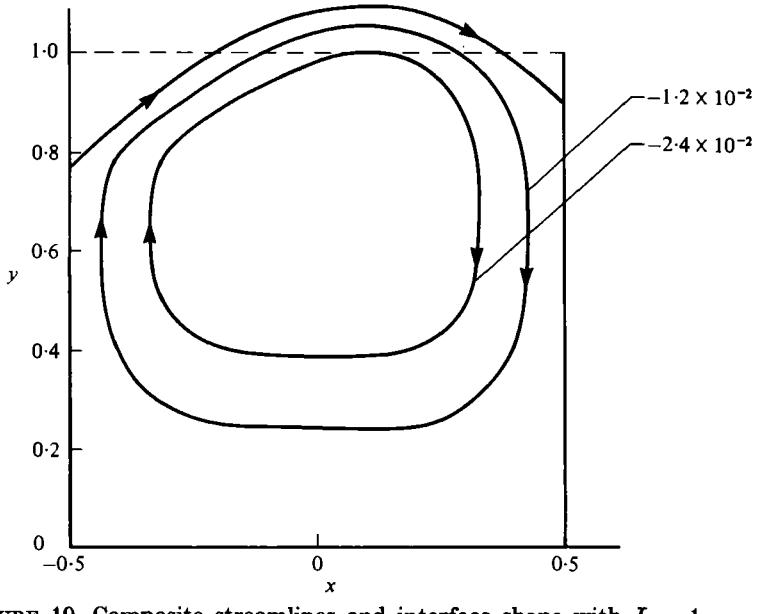

FIGURE 10. Composite streamlines and interface shape with $L = 1$, $A = 0{\cdot}2$ and $m = 1$ for case II.

parameter values as in §4, except that now $\bar{C} = 5$. The composite streamlines and the interface shape correct to $O(A^2)$ are plotted in figures 9 and 10 for the cases when $m = 0$ and $m = 1$ respectively. The former case corresponds to the interface contacting the end walls at right angles. Figures 11 and 12 show the $O(A)$ perturbations of the outer stream functions for $m = 0$ and 1 respectively.

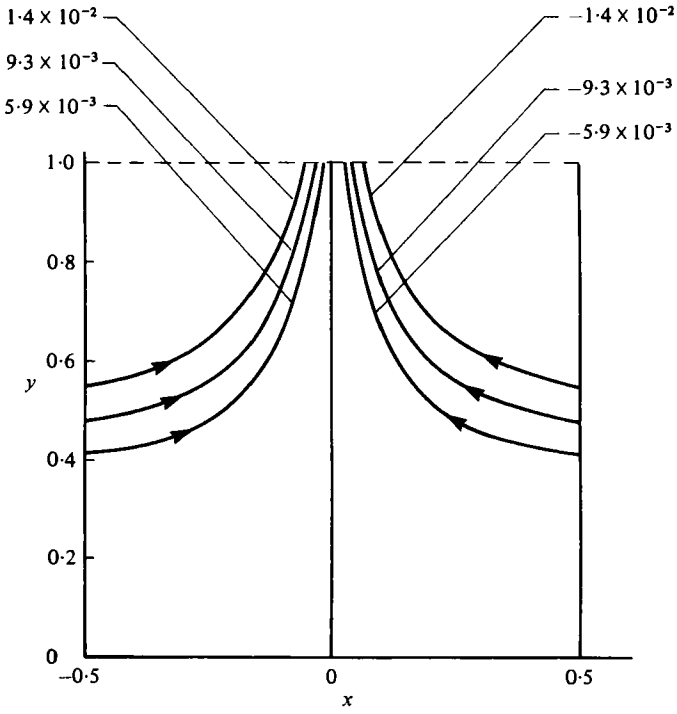

FIGURE 11. Order-A outer streamlines with $L = 1$, $A = 0{\cdot}2$ and $m = 0$ for case II.

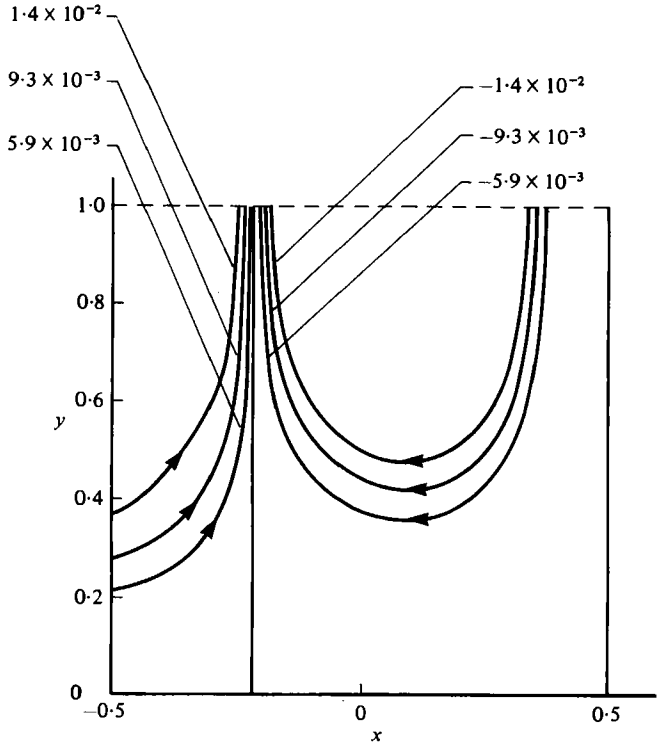

FIGURE 12. Order-A outer streamlines with $L = 1$, $A = 0{\cdot}2$ and $m = 1$ for case II.

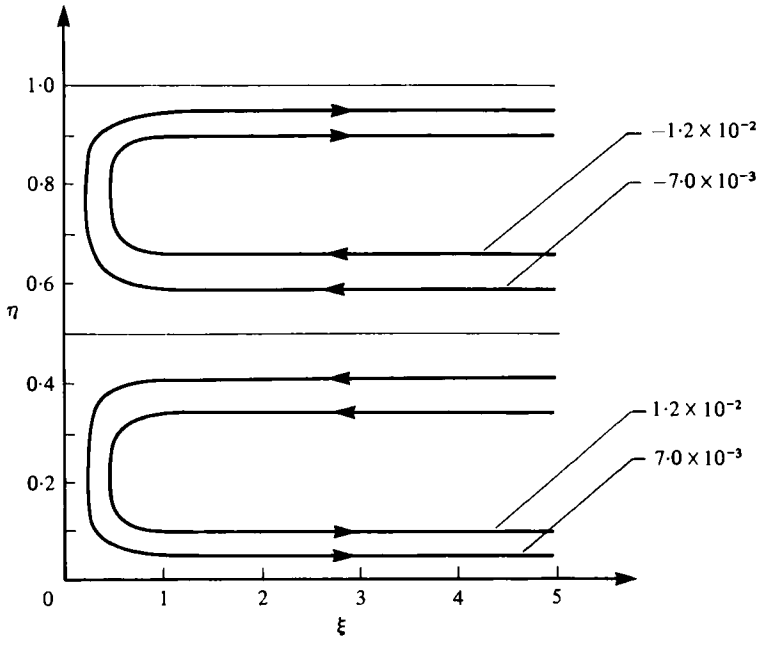

FIGURE 13. Leading-order streamlines in the left boundary layer for slot flow with two interfaces with $L = 1$ for case I (and case II).

6. Cavity with two interfaces

Consider a cavity having solid isothermal walls at $x = \pm\frac{1}{2}$, but two liquid–gas interfaces at mean positions $y = 0$ and $y = 1$. The flow patterns can be constructed from the previous analyses by using symmetry conditions about $y = \frac{1}{2}$. For example the leading-order outer velocity field is given by

$$\psi \sim \tfrac{1}{6}y(y-1)(2y-1). \tag{6.1}$$

When the interfaces are pinned at $y = 0$ and $y = 1$, as given by the conditions (2.27), then we have a version of case I. We write

$$h_{\text{upper}} \sim 1 + Ah_1(x), \quad h_{\text{lower}} \sim -Ah_1(x), \tag{6.2}$$

where

$$h_1(x) = -\tfrac{1}{3}\bar{C}x(x^2-\tfrac{1}{4}). \tag{6.3}$$

When the interfaces have given contact angles at $y = 0$ and $y = 1$, as given by the conditions (5.2), then we have a version of case II. We write forms (6.2), where now

$$h_1(x) = -\tfrac{1}{12}\bar{C}\{x(4x^2-3)+\tfrac{4}{3}m(12x^2-1)\}. \tag{6.4}$$

The core temperature in either case I or case II is

$$T \sim -x + A^2T_2 + O(A^3), \tag{6.5a}$$

where

$$T_2 = -\tfrac{1}{48}\bar{M}\left\{3y^4-4y^3+\frac{1}{L+2}(Ly+1)\right\}. \tag{6.5b}$$

Note that T_2 now depends on L.

The analysis of the boundary-layer flows is similar to that carried out in §§4 and 5, and will not be presented here. The leading-order streamlines in the left boundary layer are shown in figure 13 for both cases I and II. The composite streamlines and

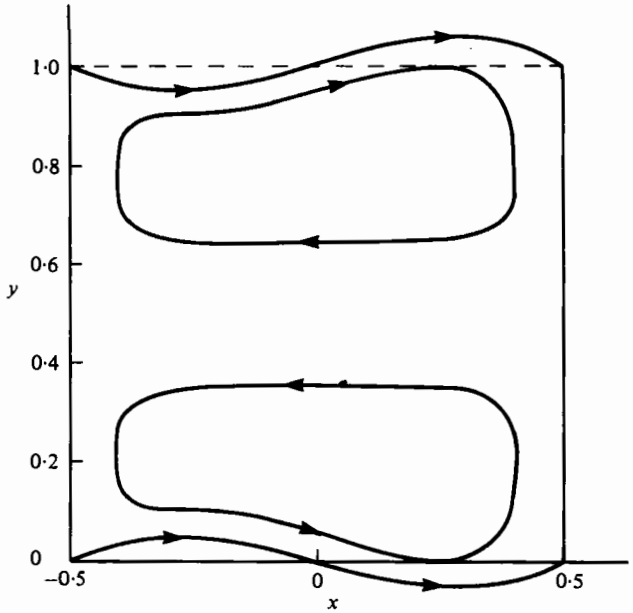

FIGURE 14. Composite streamlines and the interface shape to order A^2 for slot flow with two interfaces with $L = 1$ and $A = 0{\cdot}2$ for case I.

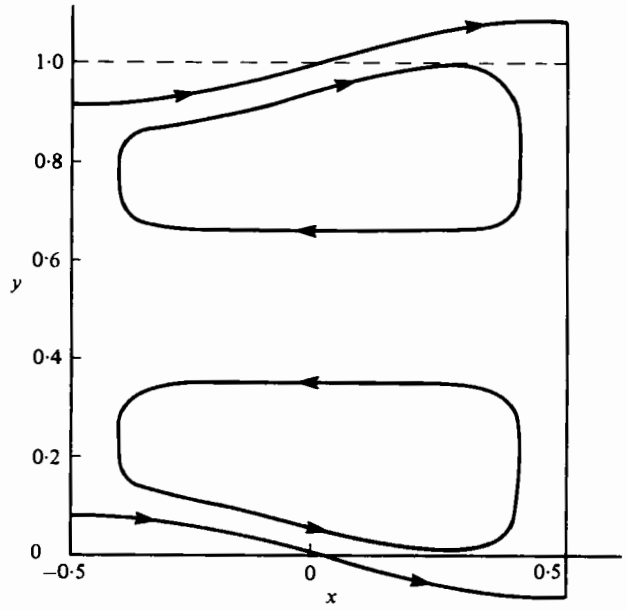

FIGURE 15. Composite streamlines and the interface shape to order A^2 for slot flow with two interfaces with $L = 1$, $A = 0{\cdot}2$ and $m = 0$ for case II.

the interface shape for case I are plotted in figure 14. Figures 15 and 16 present the composite streamlines and interface shapes for case II with $m = 0$ and $m = 1$ respectively. Again, the limit $L \to 0$ is regular, and the results for $L = 0$ are qualitatively similar to those shown for $L = 1$.

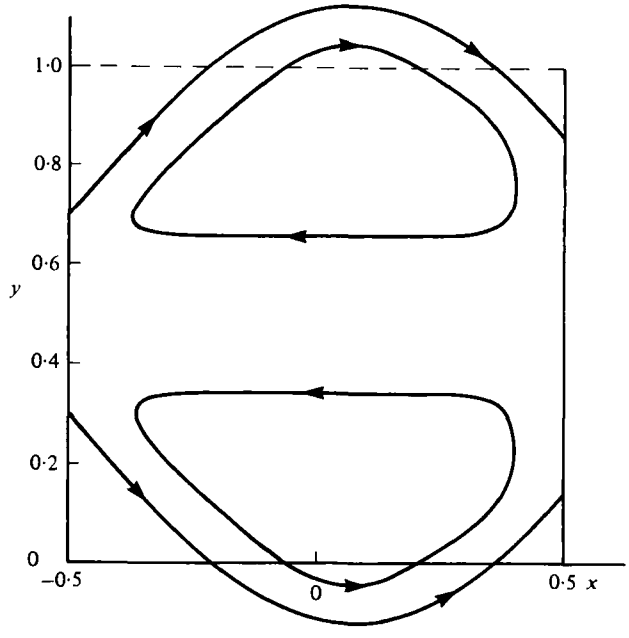

FIGURE 16. Composite streamlines and the interface shape to order A^2 for slot flow with two interfaces with $L = 1$, $A = 0{\cdot}2$ and $m = 1$ for case II.

7. Comments on results for $R = O(1)$ and $M = O(1)$

The previous work was based on the assumption that to leading order both the convective and advective nonlinearities of the governing equations of the core flow were negligible, viz $R, M = O(A)$. Consider, say, the case of the slot having a single liquid–gas interface and the contact lines pinned (case I). Let us relax the above assumptions so that $R, M = O(1)$ as $A \to 0$. If we still seek a leading-order core solution consisting of a flat top and parallel flow, then we obtain the *same* stream function ψ_0, given by (3.6), and the same temperature distribution T_0, given by (3.5).

At the next order, however, the outer temperature field is given by

$$T_1 = -\tfrac{1}{48}M(3y^4 - 4y^3 + 1), \tag{7.1}$$

which is the same distribution as given in (3.20), but it now appears at an earlier order. Hence thermal boundary layers are now present at $O(A)$. Furthermore, the boundary-layer corrections for ψ and T, given by (4.2) with $\bar{R}A$, $\bar{M}A = O(1)$, are governed by *nonlinear* balances between diffusion and convection/advection. There is a further tight coupling between the boundary-layer temperature correction $\tilde{T}_1$ and the leading-order stream function $\tilde{\psi}_0$ through the shear-stress condition (4.9g) and the bulk temperature equation (4.2b). Thus a solution for $R = O(1)$, $M = O(1)$ having a flat top and parallel flow for the leading-order core solution should exist, though the complete matching process poses a significant numerical problem.

8. Discussions and conclusions

We have analysed liquid flows in slots whose ends are maintained at fixed temperature differences. The flows are driven by thermal differences in surface tension on the liquid–gas interfaces. The flows on the interfaces are directed from the hot towards the cold end, and return along a region removed from the interfaces. The ends cause return flows by inducing axial pressure gradients. These pressure gradients determine the deflection of the liquid–gas interfaces due to the balance between normal stress (mainly the pressure) and the surface tension times the curvature.

Four cases have been analysed. The first two are slot flows having one interface and one solid surface as shown in figure 2. Here either the contact lines are fixed or the contact angles are fixed. The second two are slot flows having two interfaces where either the contact lines are fixed or the contact angles are fixed.

The analyses are of lubrication type, where we let the Reynolds and Marangoni numbers be $O(A)$ and the capillary number be $O(A^4)$ and seek asymptotic solutions for $A \to 0$ having in the core parallel flow and flat interfaces at leading order. At leading order there is a *constant* axial pressure gradient. Corrections to the core solutions have non-parallel flow and surface deformation. The core solutions can be fully determined only by matching these outer solutions to inner solutions in the end regions where the end walls cause the flows to turn. It is in these end regions that the contact-line conditions have their effects. Since $R = O(A)$ and $M = O(A)$, the whole flow is conduction-dominated at leading order, while corrections give the effects of convection and advection.

In all four cases considered, the flows are quite insensitive to the surface Biot numbers L, and in particular the limit $L \to 0$, which is often a good approximation to the case of heat loss from a liquid to a gas, is regular.

In all four cases, the leading-order pressure gradient is directed from the hot end towards the cold end. Hence the pressure is higher at the cold end, and the interface thus bulges near the cold end and is constricted near the hot end. If the contact lines are fixed, then the interface shapes are shown in figure 6. The bulges and constrictions are $O(A\bar{C})$ and the dynamic contact angles (in physical variables) are $O(A^2\bar{C})$. If the slopes are fixed at $O(Am\bar{C})$, then the interface shapes are shown in figures 9 and 10 and the contact lines are displaced by $O[(1-\frac{8}{3}m)A\bar{C}]$. It is not surprising that for large-enough surface tension (i.e. small-enough C) surface deflection can be neglected. However, the analysis shows that C must be smaller than $O(A^4)$ before this happens. This is an exceedingly small value. Even for the numerical case illustrated, using the relatively large value $A = 0{\cdot}2$, C must be smaller than 2×10^{-3}. The outer flow is a parallel flow having a parabolic profile plus $O(A)$ corrections, while the temperature field is linear in axial co-ordinate plus $O(A^2)$ corrections. The leading-order outer solutions having parallel flow and flat interfaces continue to be the leading-order outer approximations even when the conditions $R, M = O(A)$ are relaxed. Such solutions have been discussed in §7.

The present analysis gives information about the local interfacial shape at, say, the cold end. This shape depends on the wetting properties of the liquid (i.e. the contact-line conditions). Clearly, these results must be used with caution in application to the float-zone geometries shown in figure 1, where the local angles affect the crystal surface energy and hence the physical characteristics of the formed crystal. On one

hand the present analysis omits the added $O(1)$ contribution to the mean curvature that would be present in the *axisymmetric* float-zone geometry. Davis *et al.* (1974) show that, even if one has a *thin* cylindrical liquid shell, this modified curvature can greatly influence the flow. On the other hand, the present work omits changes of volume normally present during solidification. Such changes could greatly affect local interfacial shapes and hence local dynamical contact angles.

This work was supported through a contract no. NAS8-33881, National Aeronautics and Space Administration, Materials-Processing-in-Space Program.

REFERENCES

ADLER, J. 1970 *Combust. Sci. Tech.* **2**, 105.

ADLER, J. & SOWERBY, L. 1970 *J. Fluid Mech.* **42**, 549.

BABSKIY, V. G., SKLOVSKAYA, I. L. & SKLOVSKIY, Y. B. 1973 *Space Studies in the Ukraine, No.* 1: *Space Materials Studies and Technology* (ed. G. S. Pisarenko), p. 121. Kiev Nankova Domka.

BIRIKH, R. V. 1966 *J. Appl. Mech. Tech. Phys.* **7**, 43.

CORMACK, D. E., LEAL, L. G. & IMBERGER, J. 1974 *J. Fluid Mech.* **65**, 209.

DAVIS, S. H., LIU, A.-K. & SEALY, G. R. 1974 *J. Fluid Mech.* **62**, 737.

LEVICH, V. G. 1962 *Physicochemical Hydrodynamics*, p. 384. Prentice-Hall.

OSTRACH, S. 1977 *Physicochemical Hydrodynamics, V. G. Levich Festschrift* (ed. D. B. Spalding), vol. 2, p. 571. Advance.

SIRIGNANO, W. A. & GLASSMAN, I. 1970 *Combust. Sci. Tech.* **1**, 370.

TORRANCE, K. E. 1971 *Combust. Sci. Tech.* **3**, 133.

YIH, C.-S. 1968 *Phys. Fluids* **11**, 477.

YIH, C.-S. 1969 *Phys. Fluids* **12**, 1982.